WARPING STRESSES AND DEFLECTIONS IN CONCRETE PAVEMENTS - PART II

FEBRUARY 1960

NO. 5

by

J.F. WISEMAN
M.E. HARR
G.A. LEONARDS

Joint Highway Research Project

PURDUE UNIVERSITY
LAFAYETTE INDIANA

Technical Paper

WARPING STRESSES AND DEFLECTIONS IN
CONCRETE PAVEMENTS - PART II

TO: K. B. Woods, Director
Joint Highway Research Project

March 2, 1960

FROM: H. L. Michael, Assistant Director
Joint Highway Research Project

File: 9-7-2
Project: C-36-63B

Attached is a technical paper entitled, "Warping Stresses and Deflections in Concrete Pavements - Part II" and authored by J. F. Wiseman, M. E. Harr and G. A. Leonards.

The paper is a summary of additional work which has been performed by the authors on the stresses and deflections of concrete slabs on ground subjected to temperatures and/or moisture contents which decrease linearly with the depth of the slab. The paper was prepared for presentation at the Highway Research Board meeting in January of 1960.

The Joint Highway Research Project did not participate in the cost of this project, but the results are presented to the Board as information because of their interest in this research.

Respectfully submitted,

H. L. Michael

H. L. Michael, Secretary

HLM:lmc

Attachment

cc: F. L. Ashbaucher
J. R. Cooper
W. L. Dolch
W. H. Goetz
F. F. Havey
G. A. Hawkins (M. B. Scott)
G. A. Leonards
J. F. McLaughlin
R. D. Miles
R. E. Mills
C. E. Vogelgesang
J. L. Waling
J. E. Wilson
E. J. Yoder

Digitized by the Internet Archive
in 2011 with funding from
LYRASIS members and Sloan Foundation; Indiana Department of Transportation

http://www.archive.org/details/warpingstressesd02wise

Technical Paper

WARPING STRESSES AND DEFLECTIONS IN CONCRETE PAVEMENTS - PART II

by

J. F. Wiseman
M. E. Harr
and
G. A. Leonards

Joint Highway Research Project
File: 9-7-2
Project: C-36-63B

Purdue University
Lafayette, Indiana

March 2, 1960

INTRODUCTION

In their discussion of pavement warping on the [illegible] Road, Teller and Sutherland (5)* state:

> "The relation between the warping of the slab and the distribution of reactions is readily apparent. In the morning with the edges of the slab warped upward, the greatest (subgrade) pressure measured was in the interior, the pressure toward the edge being at its minimum at this time. During the day, as the upper surface of the slab expands, there is a complete relief of the high pressure in the interior region and a development of a maximum reaction near the edge exceeding the maximum previously developed in the interior by 50 percent.
>
> Both the warping data and the subgrade pressure data [illegible] the possibility of an actual lifting of the central area from the subgrade as the edges warp downward."

Harr and Leonards (1) have extended Westergaard's analysis for warped slabs to allow for the possibility that warping results in only partial support of the slab by the foundation. A complete solution was obtained for the case where the temperature and/or moisture contents increase linearly with the depth of the slab. More recently, Leonards and Harr (2) expanded their theory to include the effects of superimposed uniform loads, and axialsymmetric peripheral and point loads. In their earlier work, it was suggested that the basic theory be amplified to study the effects of warping and pavement support induced by temperatures and/or moisture contents which decrease with the depth of the slab.

In this paper, solutions have been obtained for the contact stresses and degree of support of concrete pavements subjected to temperatures and/or moisture contents which decrease linearly with the depth of the slab, and are of sufficient magnitude to raise the central portion of the slab off its foundation. Data from a controlled experiment on a 12' x 25' slab are reported and compared with predictions made from the new theory.

---

*Numbers in parentheses refer to references in Bibliography

THEORY

Assumptions

1) Slab is of circular shape, homogeneous and isotropic with a free edge boundary.

2) Slab is supported on a homogeneous foundation.

3) Reaction between slab and foundation at any point of contact is proportional to the down and deflection of the foundation at that point.

4) Slab obeys Hooke's law.

5) Deflections of the slab are small in comparison with its thickness which is constant.

6) External forces acting of the slab are those due to gravity only.

7) Slab is subject to ambient changes in temperature and/or moisture content which decrease linearly with the depth of the slab but are constant on all planes parallel to the upper and lower slab surfaces.

Formulation of Problem

The specific solution developed herein pertains to the case where the temperature and/or moisture content decrease linearly with the depth of the slab. Consequently, the edges of the pavement will tend to warp down. The slab is divided into two zones (Figure 1) with the inner portion (zone 1) being a uniformly loaded slab unsupported by the foundation.

Conditions of continuity require that along the circle of radius a the deflection, slope, bending moment, and shear of both the inner and outer portions be equal.

As the load and reactive forces are symmetrically disturbed about an axis perpendicular to the slab through its center, both the slope and the shear at the center of the slab must be zero.

The assumptions, boundary conditions, and symmetry may be summarized as follows (nomenclature is listed in Appendix I):

a) $w_1'(0) = 0$

b) $V_1(0) = 0$

c) $w_1(b) = 0$

d) $w_2(b) = 0$

e) $V_2(a) = 0$

f) $M_2(a) = 0$

g) $w_1'(b) = w_2(b)$

h) $M_1(b) = M_2(b)$

i) $V_1(b) = V_2(b)$

j) $w_1(0) \leqq 0$

Applying the conditions listed above to the governing differential equations, equations for stresses and deflections in the slab are obtained (Appendix [illegible]).

RESULTS

As was the case for upward warping, a prohibitive amount of work would be involved in eliminating the constants and obtaining an explicit expression for either the stresses or deflections in terms of the slab parameters. Hence, a high speed computer was used to obtain the desired information.

The derived equations were solved for deflections and maximum radial stresses for various combinations of the following:*

$E = 3 \times 10^6, 4 \times 10^6, 5 \times 10^6$ psi

$a = 120", 150", 180", 210", 240"$

$h = 6", 8", 10", 12", 14", 18", 30", 48"$

$K = 100, 200, 400,$ pci

$\alpha = 6 \times 10^{-6}$ inches per inch per degree F

$\mu = 0.15$

---

* [illegible]

Typical [illegible] curves for representative conditions are shown in Figure 2. Corresponding radial stresses as a function of radial [illegible] from the center of the slab are shown in Figure 3.

[illegible] relationships are shown in the form of charts [illegible]. These relationships are plots of the [illegible] to the modulus of rupture (M_r) for effective [illegible] of 20°F, 30°F, and 40°F and for various [illegible] radii (a) and thicknesses (h). The use of these [illegible] illustrated in an example. For a stress ratio ([illegible]) [illegible] E [illegible] 10[illegible] psi, T = 100 psi and with an anticipated effective [illegible] difference of 30°F, (following the arrows in Figure 4) [illegible] among the various possible solutions are a 151" [illegible] 9" thick, and 231" radius slab 18" thick.

[illegible] curves for different values of h in Figure 4, followed [illegible] was decided to calculate the curve for h = 14" only [illegible] number of causes and estimate it for the remaining cases [illegible] the h = 14" curve is shown dotted in Figures 4.

[illegible] for a = 240", T = 30°F are cross-plotted on Figure 5 to [illegible] the effects of the quality of the concrete in the slab as [illegible] to the modulus of elasticity, E.

DISCUSSION OF RESULTS

Examination of Assumptions

The assumptions that the slab was circular, and had a free edge boundary, have already been examined (1) and found valid for unloaded slabs of a size of interest in the design of concrete pavements.

The no-support condition under the central portion of the slab (zone 1, Figure 1) imposes a necessary but insufficient condition. In

the prototype, the downward displacement of the center of the slab below the ground line would be resisted by the base. In the theoretical model it is possible for the central portion of the slab to be below the original ground line for two conditions: 1) when a large portion of the slab is unpolished and the slab is sufficiently flexible to permit its central portion to deflect beneath the original ground line, and 2) when the applied temperature gradient is insufficient to lift any part of the slab above the original ground line. Thus, it was necessary to specify that the deflection at the center of the slab be above the original reference line $\left[w_1(0) \leq 0\right]$. This condition accounts for the limited range of some of the effective temperature curves in Figures 44 to 48. For example: for a slab radius a 240", $E = 3 \times 10^6$ psi, $\lambda = 100$ pci (Figure 46), thicknessess of less than 14" and effective temperature differences between slab surfaces of 30°F or less, the deflection at the center of the slab is below the ground line and the analysis is invalid. For the same conditions with a large slab thickness, (h = 34" ±) a temperature difference of 20°F is insufficient to cause any portion of the slab to warp up to the ground line.

COMPARISON WITH OTHER THEORETICAL DATA

Comparing stresses in slabs subjected to upward warping with those that develop in downward warping, it is found that for equivalent slab parameters and effective temperature differences, the maximum stress in the former case is generally somewhat higher than in the latter. A typical comparison is shown in Table 1. It is apparent that the differences in maximum radial stresses are not great, and both downward and upward warping can be about equally destructive.

TABLE I

Comparison of Theoretical Data
for Different Size Slabs

E = 5,000,000 psi
K = 100 pci
T = 30°F

h	a = 120"			a = 180"			a = 240"		
Inches	I*	II**	III***	I	II	III	I	II	III
3	.450	.270	36.0	.725	.600	17.2	.730	—	—
6	.350	.205	32.6	.635	.450	29.2	.745	.795	- 6.7
10	.220	.165	25.0	.510	.355	30.4	.725	.640	11.7
14	.125	.125	0.0	.350	.245	30.0	.590	.450	23.7
18	.060	.060	0.0	.250	.185	26.0	.450	.330	26.7

COMPARISON WITH OBSERVED MEASUREMENTS

A 12 x 25 ft. x 6 in. portland cement concrete slab was constructed on a soil-cement subbase by the Portland Cement Association at their Skokie, Ill., laboratory. The slab was instrumented to measure temperatures, deflections, and the degree of unsupport, and was continuously inundated to prevent the development of moisture gradients. Temperature differences between slab surfaces were induced either with an ice slush or by circulating hot water over the surface of the slab. Temperatures and deflections were measured continuously until a linear temperature variation was obtained.

The conic modulus of the concrete in the slab was evaluated to be 5,000,000 psi and the initial modulus of subgrade reaction for the soil cement subbase was measured to be between 360 and 400 pci.

Three types of deflection readings were taken: 1) movement of the slab relative to the subbase, 2) movement of the slab relative to a bridge above the slab surface supported on the floor of the laboratory,

* I is %/hr for upward warping.
** II is %/hr for downward warping.
*** III is percent difference [(I-II)/I] x 100

[illegible] of the slab relative to deep rods anchored below the surface. Deflections were measured at the top of the slab and at 1½ inch intervals up the depth of the slab. The location of the deflection measuring devices is shown in Figure 6. Figure 7 shows the instrumented slab during the test.

In Figure 8, measured deflections (dotted curve) are compared with the computed deflections (solid curve) for a circular slab with a radius equal to the length of the diagonal of the rectangular slab, a slab modulus of elasticity of 4,500,000 psi, a modulus of subgrade reaction of 400 psi, and an effective linear temperature gradient varying with the depth of the slab, of 20°F. In Figure 9, measured deflections are compared with the computed deflections of the same slab, calculated using a slab modulus of elasticity of 4,000,000 psi, a modulus of subgrade reaction of 400 psi, and an effective linear temperature gradient that increases with the depth of the slab, of 16°F.

The validity, between the measured and theoretical deflection curves, as shown in Figures 8 and 9, offers substantial evidence regarding the validity of the theory as applied to linear temperature gradients in reinforced slabs with free edges.

Effective Gradients

It was found by tests at Arlington, Va. (5) that temperature differences in the daytime (particularly in the summer after the sun had heated the upper surface of an 8" slab) reach a maximum of 4°F per inch of depth. Inspection of Figures 4A to 4I reveals that effective temperature differences between slab surfaces greater than those generally encountered in practice are required to produce tensile stresses which approach the modulus of rupture of the slabs. Thus, damaging warping stresses are likely to develop only with a critical combination of temperature and moisture gradients.

CONCLUSIONS

1. On the basis of the assumptions stated herein, the stresses, deflections and degree of support of concrete pavements subject to warping caused by linear ambient temperature and/ or moisture variation can be calculated. Comparison with measurements made under controlled conditions shows that the theory is valid under these circumstances.

2. Temperature and moisture gradients encountered in practice, when they are combine that their effects are additive, are capable of producing tensile stresses which may exceed the modulus of rupture of concrete highway slabs.

3. Rational design of concrete pavements requires that the effects of warping, including conditions of unsupport, be evaluated. This cannot be accomplished until data becomes available on the basis of which the critical moisture gradients that may develop in practice (and the volume changes that arise therefrom) can be evaluated.

BIBLIOGRAPHY

1. Harr, M. E., and Leonards, G. A., "Warping Stresses and Deflections in Concrete Pavements," Highway Research Board Proceedings, Vol. 38 (1959)

2. Leonards, G. A., and Harr, M. E., "Analysis of Concrete Slabs on Ground," Proceedings of American Society of Civil Engineers, Vol. 20, (1959)

3. Hetenyi, E., and Parkus, H., "Warmespannungen," Springer-Verlag, Vienna, (1953)

4. Schleicher, F., "Kreisplatten auf elastischer Unterlage," Julius Springer, Berlin, (1926)

5. Teller, L. W., and Sutherland, E. C., "The Structural Design of Concrete Pavements," Public Roads, October, 1935; November, 1935; December 1935; September, 1936; October, 1936; April-May-June, 1945.

6. Timoshenko, S., "Theory of Plates and Shells," McGraw-Hill, New York (1940)

7. Westergaard, H. M., "Analysis of Stresses in Concrete Roads Caused by Variations of Temperature," Public Roads, May 1927.

APPENDIX I

Nomenclature

Symbols in parentheses represent the dimensions of:

F = force
L = length
t = temperature

w = deflection, positive in the downward direction, (L)

q = distributed load due to weight of slab (F/L^2)

K = Modulus of subgrade reaction (F/L^3)

p = reaction of subgrade, $p = Kw$, (F/L^2)

h = slab thickness (L)

μ = Poisson's ratio

E = Young's modulus

$D = \frac{Eh^3}{12(1-\mu^2)}$ = the flexural rigidity of the slab (FL)

$\ell = \sqrt[4]{D/K}$ = radius of relative stiffness (L)

α = linear coefficient of thermal expansion (t^{-1})

T = temperature difference between upper and lower slab surfaces (t)

r = radial distance (L)

a = slab radius (L)

b = radial distance to point of zero deflection (L)

$\gamma = \frac{a}{\ell}$

$\beta = \frac{b}{\ell}$

$\rho = \frac{r}{\ell}$

w' = slope at point r

$$M(r) = -D\left[\frac{d^2w}{dr^2} + \frac{\mu}{r}\frac{dw}{dr} + \alpha(1+\mu)\frac{T}{h}\right]$$

= radial bending moment at point r (see ref. 3), (FL/L)

$$V(r) = -D\left[\frac{d}{dr}\nabla_r^2 w\right]$$ = shear at point r (see ref. 3), (F/L)

$\sigma(r) = \frac{E}{2(1-\mu^2)} \left[\frac{M(r)}{D} \right]$ = normal radial stress at point r, positive denotes tension (FL^{-2})

σ_0 = radial normal stress at center of slab (FL^{-2})

C_q = coefficient

$Z_q(\rho)$ = Bessel functions

$Z_q'(\rho)$ = first derivative of $Z_q(\rho)$

$\nabla^2 = \left(\frac{d^2}{dr^2} + \frac{1}{r}\frac{d}{dr}\right)$

ln = natural logarithm

APPENDIX II

The general differential equation for the deflection of a thin circular plate resting on an elastic foundation is given (4) as:

$$\nabla^4 w = \frac{q-p}{D} \qquad (1)$$

The solution of equation (1) was obtained by Schleicher (4) in the following form:

$$w = -\frac{q}{D}\left(1 + C_5 Z_1(\rho) + C_6 Z_2(\rho) + C_7 Z_3(\rho) + C_8 Z_4(\rho)\right) \qquad (2)$$

For the region where the plate is unsupported (Figure 1) equation (1) reduces to:

$$\nabla^4 w = -\frac{q}{D}. \qquad (3)$$

The solution of equation (3) is given by Timoshenko (6) to be:

$$w = C_1 + C_2 \ln r + C_3 r^2 + C_4 r^2 \ln r + \frac{qr^4}{64D} \qquad (4)$$

Solution of Problem

Applying the conditions listed on page 3 to the governing equations for stresses and deflections in the slab we find:

For $0 \leq r \leq b$

$$\sigma(r) = \frac{Eh}{2(1-\mu^2)}\left[2(\mu+1)C_3 + \frac{qr^2}{16D}(3+\mu) - \alpha(1+\mu)\frac{T}{h}\right]$$

$$w_1(r) = (r^2-b^2)\left[C_2 + \frac{q}{64D}(r^2+b^2)\right]$$

For $b \leq r \leq a$ or $\beta \leq \rho \leq \phi$

$$\sigma(\rho) = \frac{Eh}{2(1-\mu^2)}\left[\frac{q}{kd^2}\left\{C_5\left(Z_2(\rho) - (1-\mu)\frac{Z_1'(\rho)}{\rho}\right) - C_6\left(Z_1(\rho) + (1-\mu)\frac{Z_2'(\rho)}{\rho}\right) + C_7\left(Z_4(\rho) - (1-\mu)\frac{Z_3'(\rho)}{\rho}\right) - C_8\left(Z_3(\rho) + (1-\mu)\frac{Z_4'(\rho)}{\rho}\right)\right\} - \alpha(1+\mu)\frac{T}{h}\right]$$

$$w_2(\rho) = \frac{q}{K}\left(1 + C_5 Z_1(\rho) + C_6 Z_2(\rho) + C_7 Z_3(\rho) + C_8 Z_4(\rho)\right)$$

where C_3, C_5, C_6, C_7, C_8, and T may be obtained from the following equations,

$$C_5 Z_1'(\beta) + C_6 Z_2'(\beta) + C_7 Z_3'(\beta) + C_8 Z_4'(\beta) = \frac{K\ell}{q}\left(2b\,C_3 + \frac{q b^3}{16D}\right)$$

$$C_5 Z_1(\beta) + C_6 Z_2(\beta) + C_7 Z_3(\beta) + C_8 Z_4(\beta) = -1$$

$$\left\{Z_2(\beta) - (1-\mu)\frac{Z_1'(\beta)}{\beta}\right\}C_5 - \left\{Z_1(\beta) + (1-\mu)\frac{Z_2'(\beta)}{\beta}\right\}C_6 + \left\{Z_4(\beta) - (1-\mu)\frac{Z_3'(\beta)}{\beta}\right\}C_7$$
$$- \left\{Z_3(\beta) + (1-\mu)\frac{Z_4'(\beta)}{\beta}\right\}C_8 = \frac{K\ell^2}{q}\left[2(\mu+1)\,C_3 + \frac{q b^2}{16D}(3+\mu)\right]$$

$$C_5 Z_2'(\beta) - C_6 Z_1'(\beta) + C_7 Z_4'(\beta) - C_8 Z_3'(\beta) = \frac{b}{2\ell}$$

$$C_5 Z_2'(\phi) - C_6 Z_1'(\phi) + C_7 Z_4'(\phi) - C_8 Z_3'(\phi) = 0$$

$$\left\{Z_2(\phi) - (1-\mu)\frac{Z_1'(\phi)}{\phi}\right\}C_5 - \left\{Z_1(\phi) + (1-\mu)\frac{Z_2'(\phi)}{\phi}\right\}C_6 + \left\{Z_4(\phi) - (1-\mu)\frac{Z_3'(\phi)}{\phi}\right\}C_7$$
$$- \left\{Z_3(\phi) + (1-\mu)\frac{Z_4'(\phi)}{\phi}\right\}C_8 - \frac{K\ell^2}{q}\left\{\frac{\alpha(1+\mu)}{h}\right\}T = 0$$

The problem was programmed using the Purdue Compiler for the Datatron 204 digital computer.

The Bessel functions $Z_1(\rho)$ and $Z_2(\rho)$ and their first derivatives were computed from standard library subroutines. The Hankel functions $Z_3(\rho)$ and $Z_4(\rho)$ and their first derivatives were interpolated from tabular values stored in the main memory of the computer.

The main program was written with b, the radial distance to the point of zero deflection, as the independent variable; and T, the effective temperature difference between the slab surfaces, as the dependent variable.[1] Thus, by introducing a set of parameters (K, a, E, and h), the computer would solve for T corresponding to a given value of b, and then print out the stress and deflection at equal radial increments across the slab. Repeating the cycle for increasing (or decreasing) values of b, the stresses and deflections were obtained for a wide range of temperatures.

---

1) The program is on file at the Statistical Laboratory, Purdue University, Lafayette, Indiana

SIMPLIFIED DIAMETRAL SECTION OF WARPED SLAB

FIGURE 1

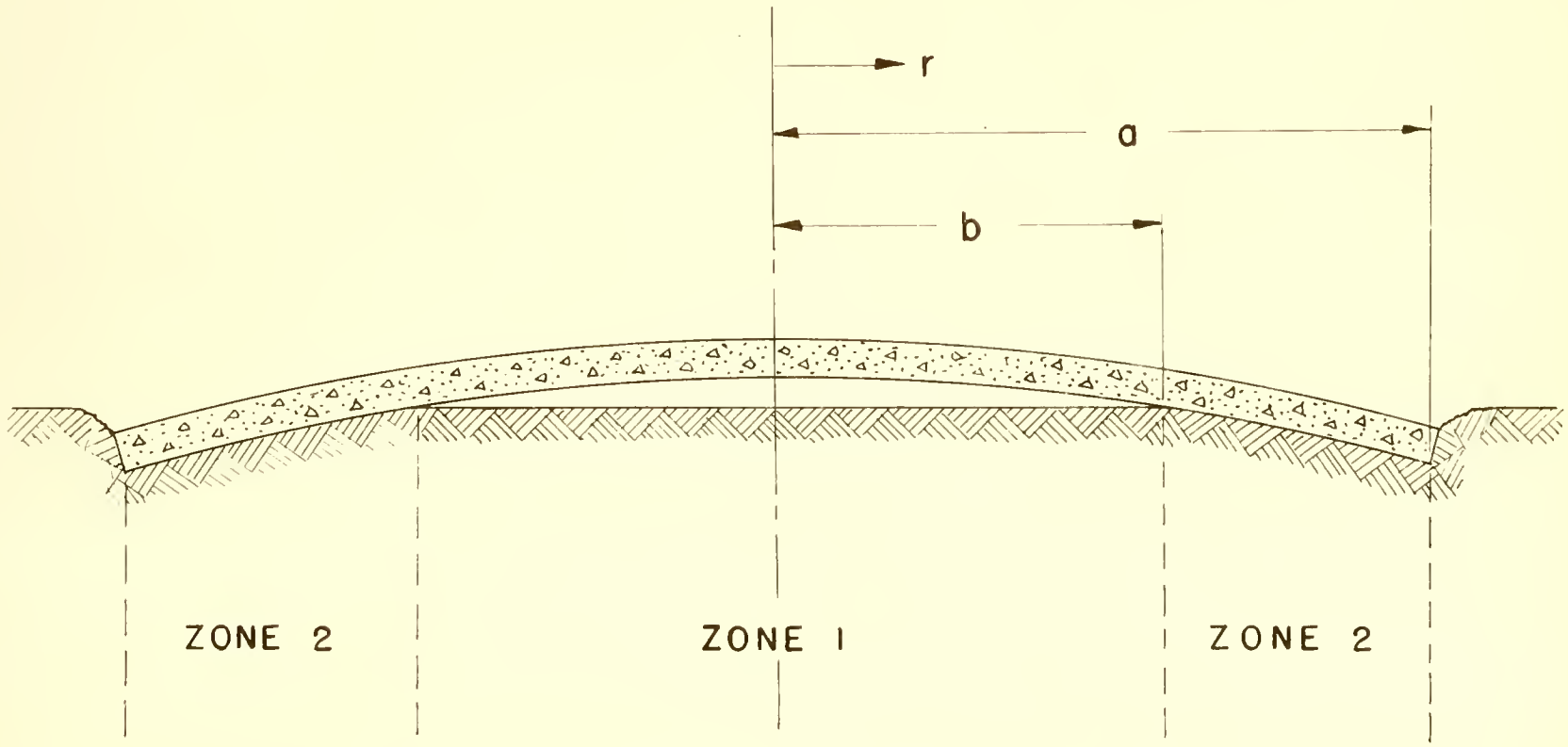

REPRESENTATIVE DEFLECTION CURVES FOR AN EFFECTIVE TEMPERATURE DIFFERENCE OF 30° F. BETWEEN SLAB SURFACES

FIGURE 2

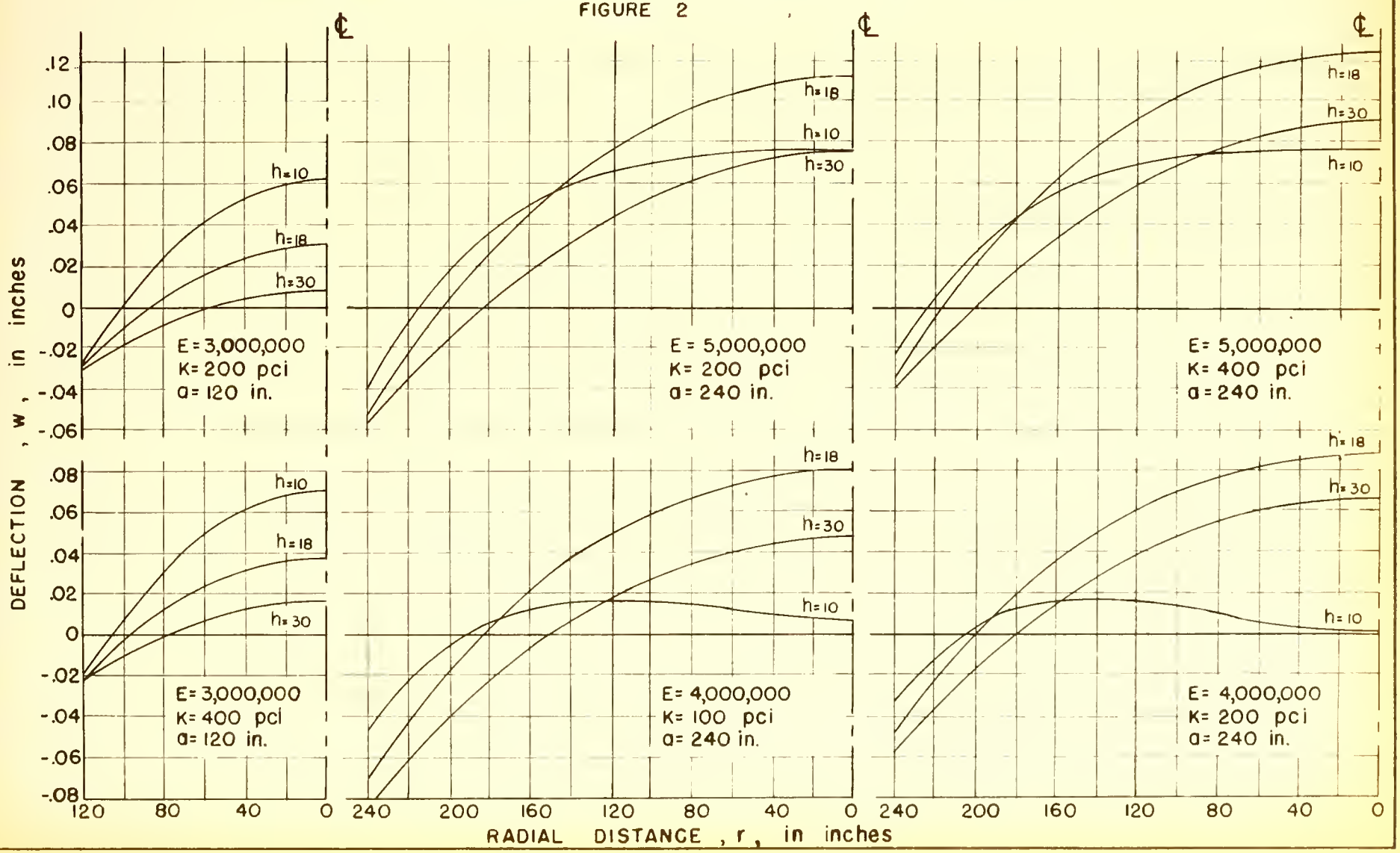

REPRESENTATIVE RADIAL STRESSES FOR AN EFFECTIVE TEMPERATURE DIFFERENCE OF 30° F. BETWEEN SLAB SURFACES

FIGURE 3

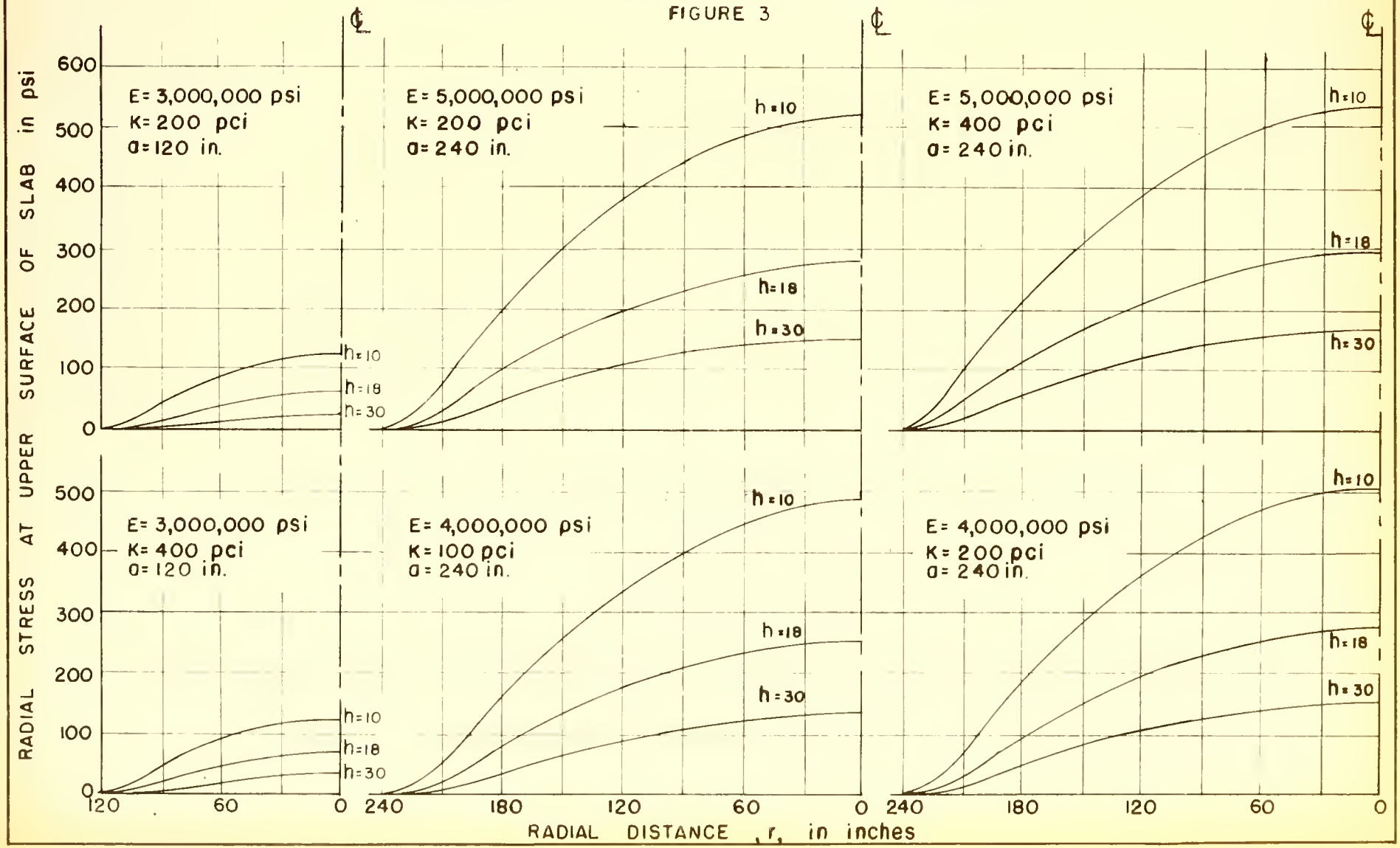

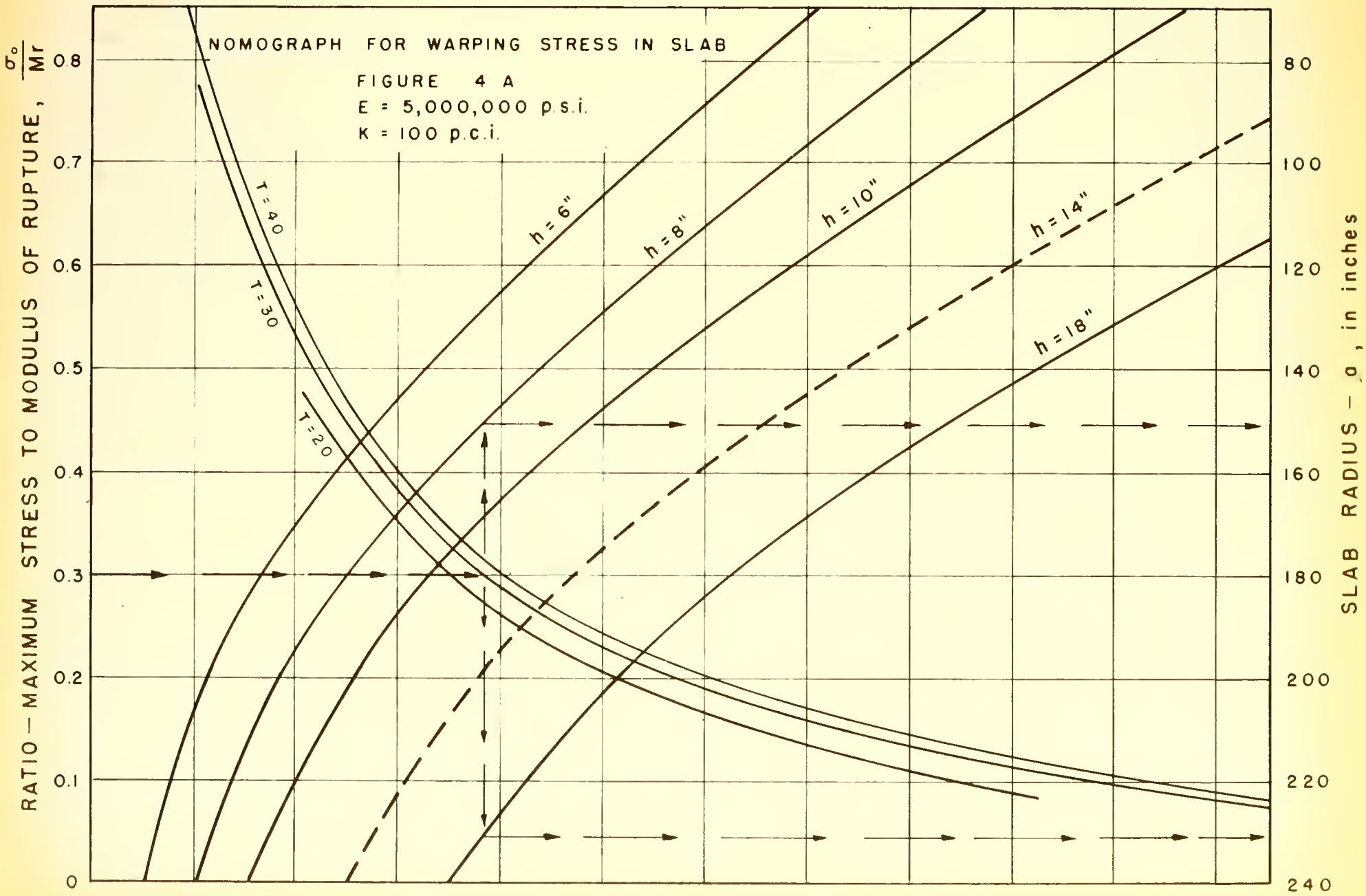
NOMOGRAPH FOR WARPING STRESS IN SLAB
FIGURE 4 A
E = 5,000,000 p.s.i.
K = 100 p.c.i.
RATIO — MAXIMUM STRESS TO MODULUS OF RUPTURE, $\frac{\sigma_o}{Mr}$
SLAB RADIUS — a, in inches
0
0.1
0.2
0.3
0.4
0.5
0.6
0.7
0.8
80
100
120
140
160
180
200
220
240
T = 40
T = 30
T = 20
h = 6"
h = 8"
h = 10"
h = 14"
h = 18"

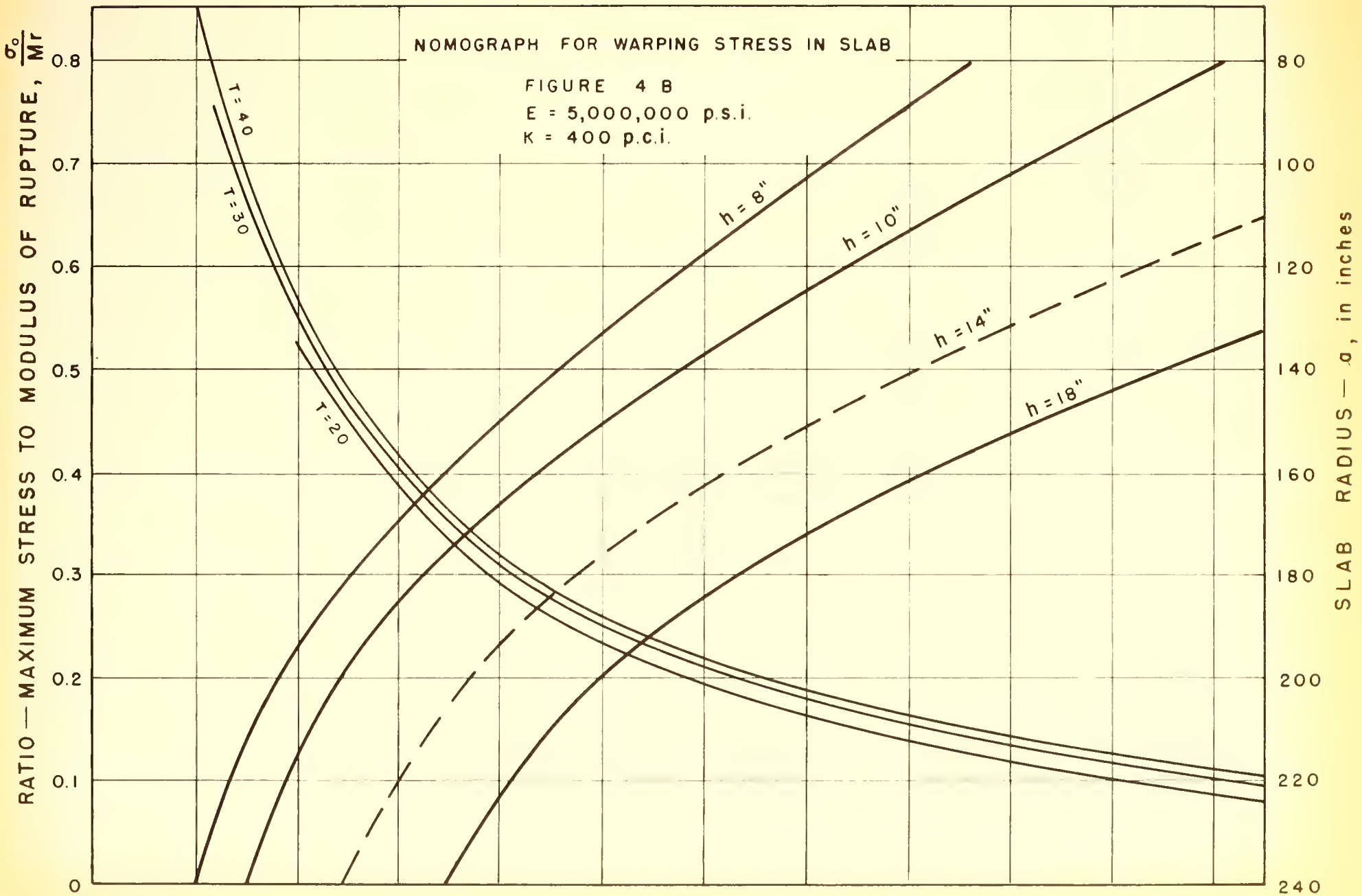
NOMOGRAPH FOR WARPING STRESS IN SLAB
FIGURE 4 B
E = 5,000,000 p.s.i.
K = 400 p.c.i.
RATIO — MAXIMUM STRESS TO MODULUS OF RUPTURE, $\frac{\sigma_o}{Mr}$
SLAB RADIUS — a, in inches
0
0.1
0.2
0.3
0.4
0.5
0.6
0.7
0.8
80
100
120
140
160
180
200
220
240
T = 40
T = 30
T = 20
h = 8"
h = 10"
h = 14"
h = 18"

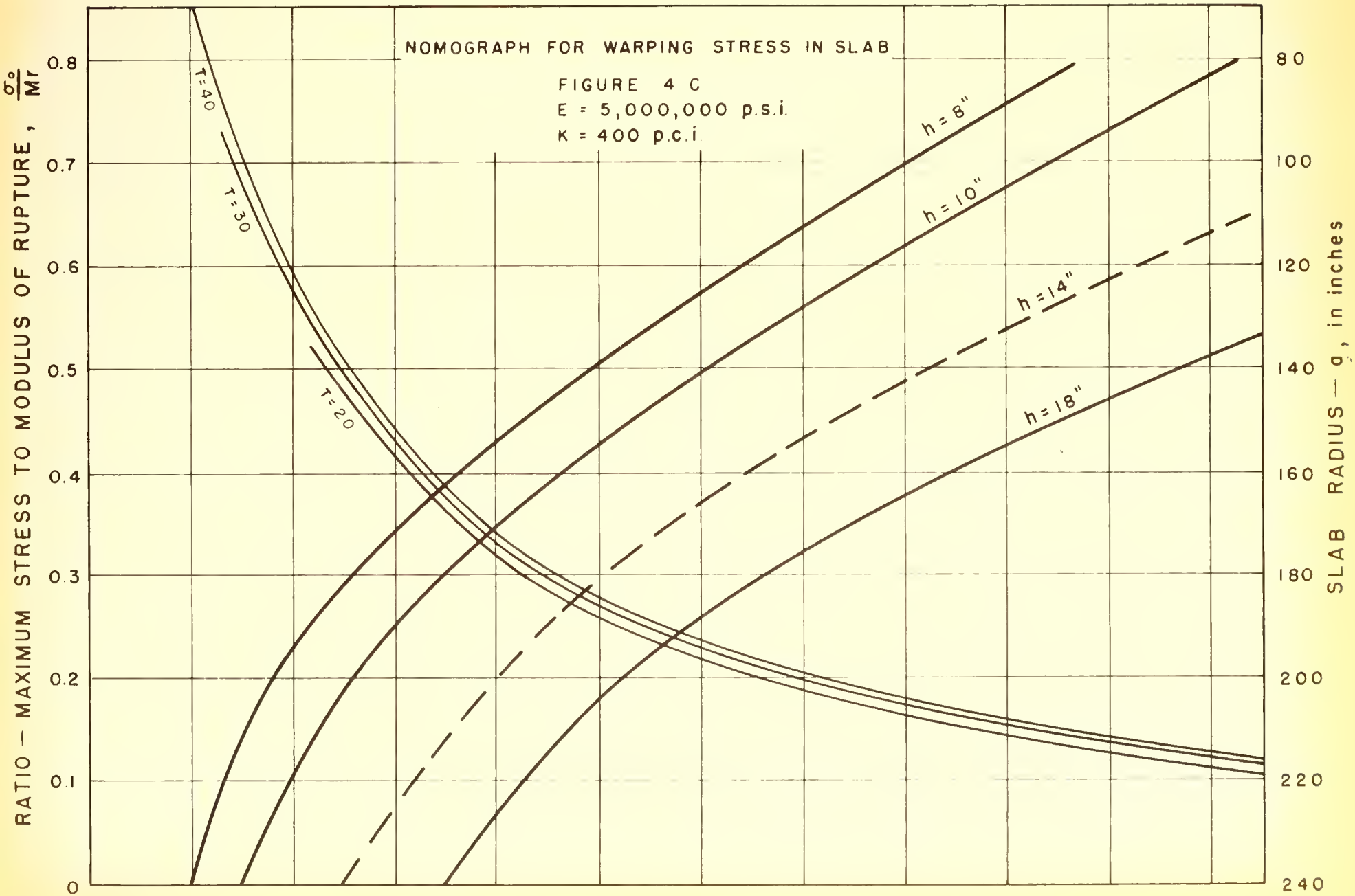
NOMOGRAPH FOR WARPING STRESS IN SLAB
FIGURE 4 C
E = 5,000,000 p.s.i.
K = 400 p.c.i.
RATIO — MAXIMUM STRESS TO MODULUS OF RUPTURE, $\frac{\sigma_o}{Mr}$
SLAB RADIUS — a, in inches
0
0.1
0.2
0.3
0.4
0.5
0.6
0.7
0.8
80
100
120
140
160
180
200
220
240
T=40
T=30
T=20
h=8"
h=10"
h=14"
h=18"

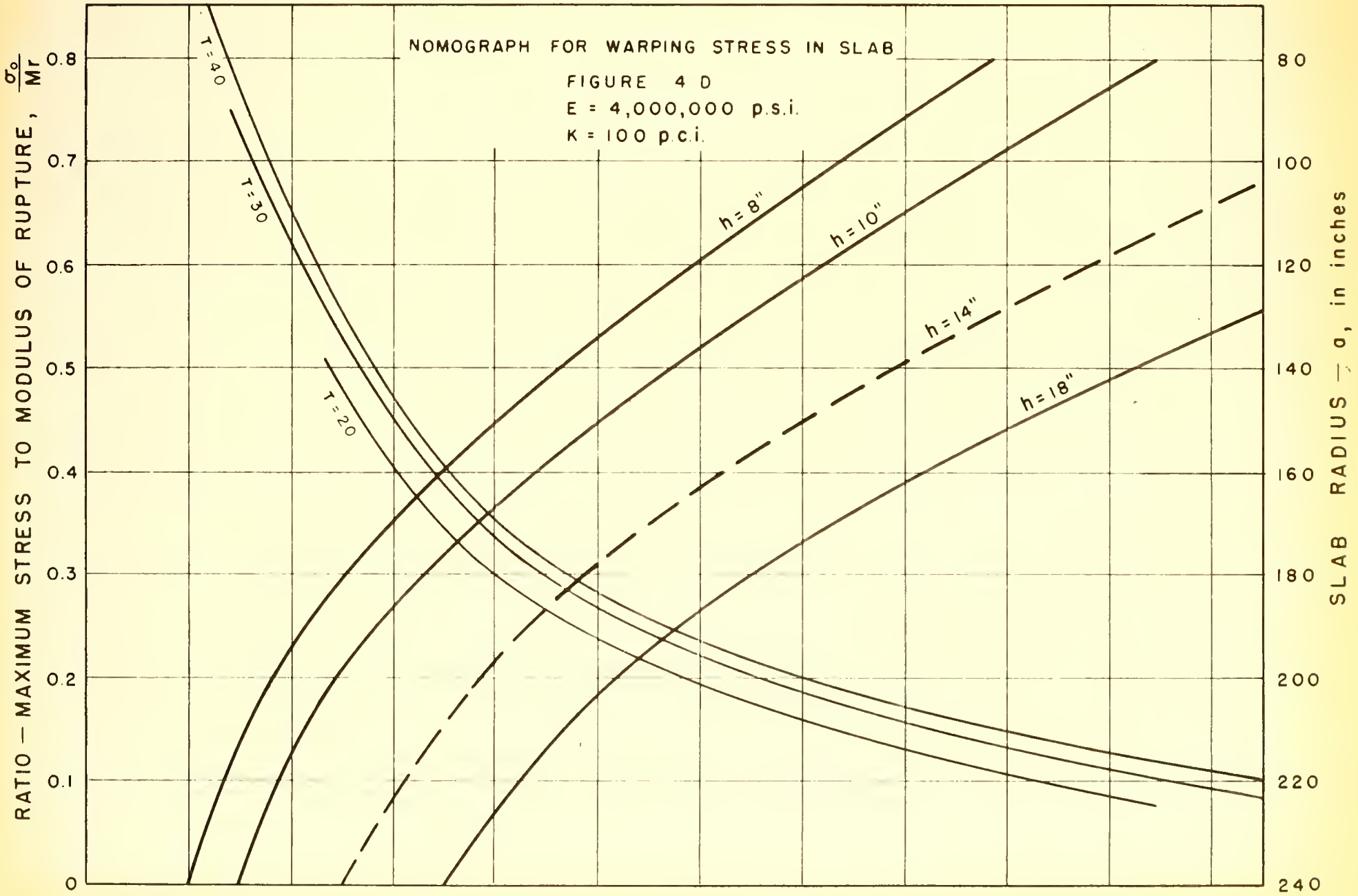
NOMOGRAPH FOR WARPING STRESS IN SLAB
FIGURE 4 D
E = 4,000,000 p.s.i.
K = 100 p.c.i.
RATIO — MAXIMUM STRESS TO MODULUS OF RUPTURE, σo/Mr
SLAB RADIUS — a, in inches
T = 40
T = 30
T = 20
h = 8"
h = 10"
h = 14"
h = 18"
0
0.1
0.2
0.3
0.4
0.5
0.6
0.7
0.8
80
100
120
140
160
180
200
220
240

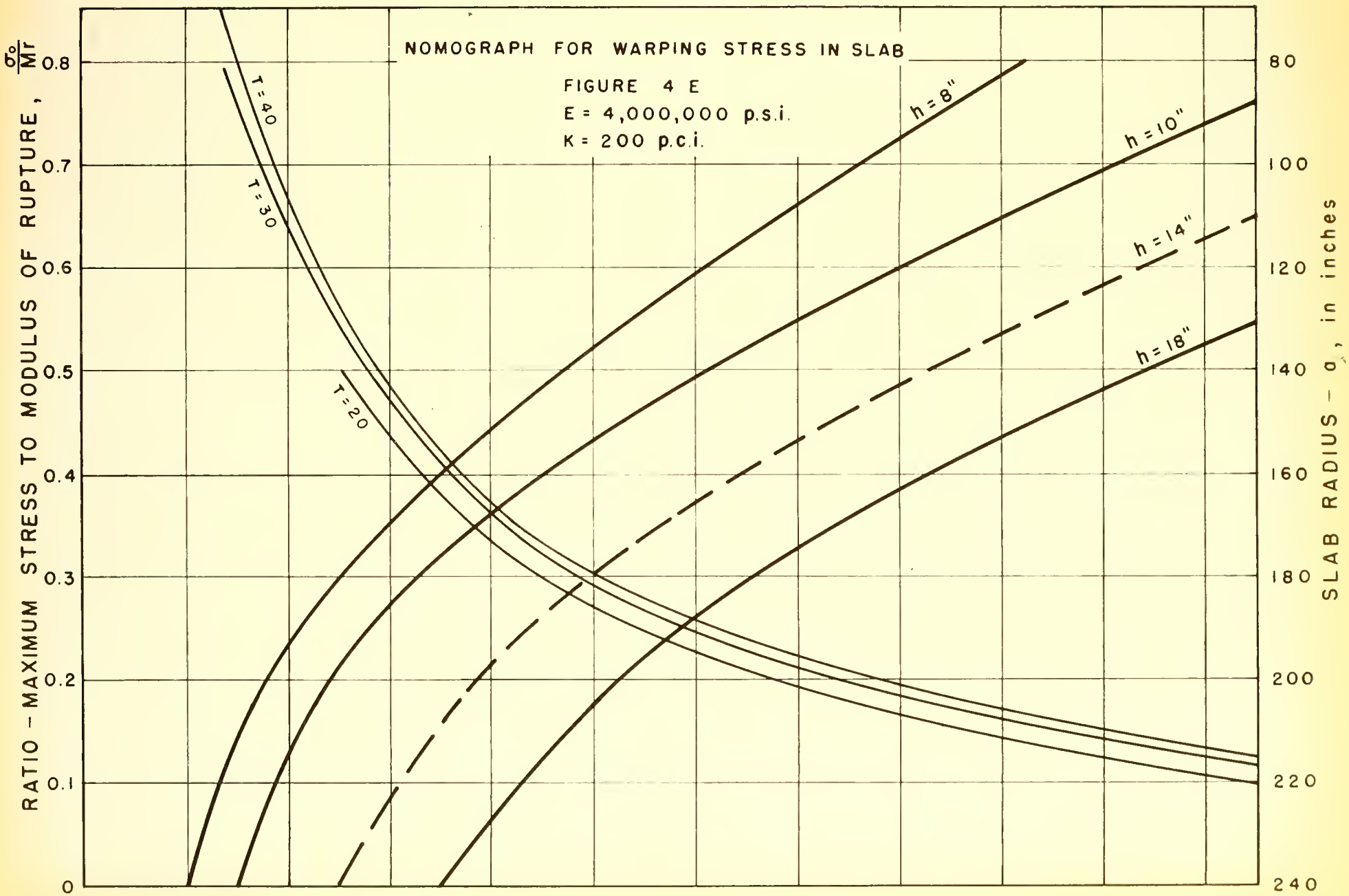
NOMOGRAPH FOR WARPING STRESS IN SLAB
FIGURE 4 E
E = 4,000,000 p.s.i.
K = 200 p.c.i.
RATIO - MAXIMUM STRESS TO MODULUS OF RUPTURE, σo/Mr
SLAB RADIUS - a, in inches
0
0.1
0.2
0.3
0.4
0.5
0.6
0.7
0.8
80
100
120
140
160
180
200
220
240
T = 40
T = 30
T = 20
h = 8"
h = 10"
h = 14"
h = 18"

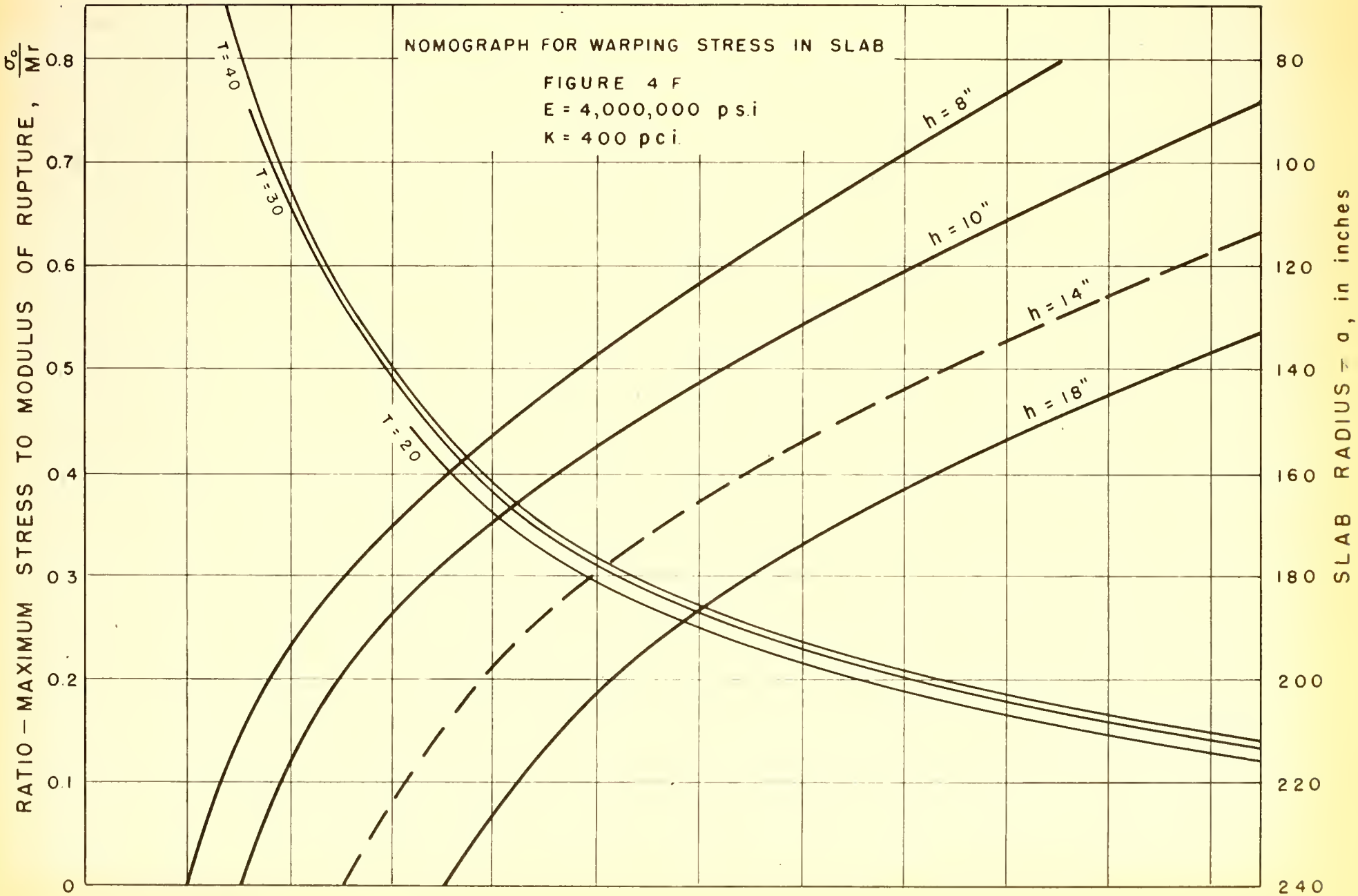
NOMOGRAPH FOR WARPING STRESS IN SLAB
FIGURE 4 F
E = 4,000,000 psi
K = 400 pci
RATIO — MAXIMUM STRESS TO MODULUS OF RUPTURE, $\frac{\sigma_o}{Mr}$
SLAB RADIUS — a, in inches
T = 40
T = 30
T = 20
h = 8"
h = 10"
h = 14"
h = 18"
0
0.1
0.2
0.3
0.4
0.5
0.6
0.7
0.8
80
100
120
140
160
180
200
220
240

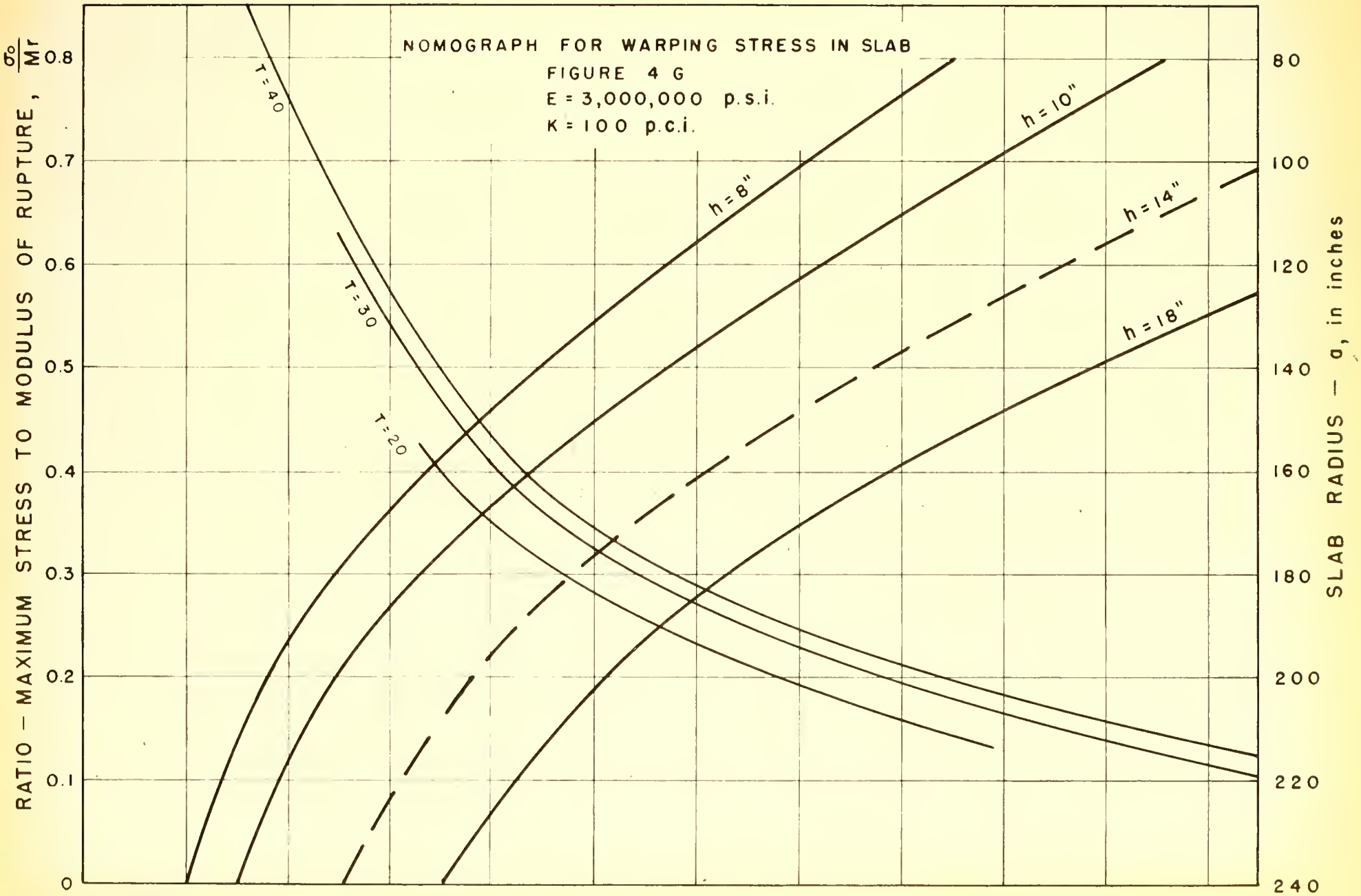
NOMOGRAPH FOR WARPING STRESS IN SLAB
FIGURE 4 G
E = 3,000,000 p.s.i.
K = 100 p.c.i.
RATIO — MAXIMUM STRESS TO MODULUS OF RUPTURE, $\frac{\sigma_o}{Mr}$
SLAB RADIUS — a, in inches
T = 40
T = 30
T = 20
h = 8"
h = 10"
h = 14"
h = 18"
0
0.1
0.2
0.3
0.4
0.5
0.6
0.7
0.8
80
100
120
140
160
180
200
220
240

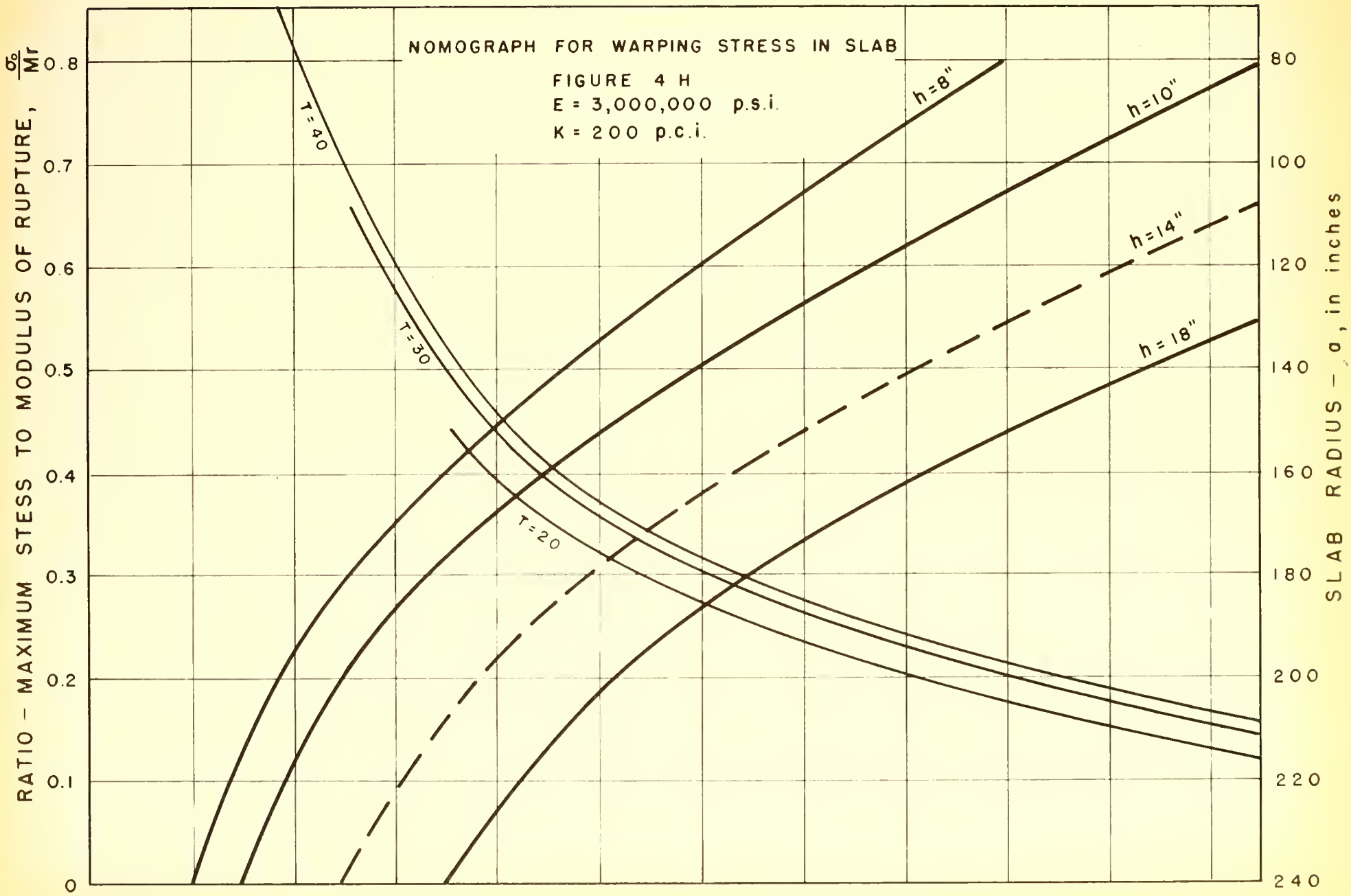
NOMOGRAPH FOR WARPING STRESS IN SLAB
FIGURE 4 H
E = 3,000,000 p.s.i.
K = 200 p.c.i.
RATIO – MAXIMUM STESS TO MODULUS OF RUPTURE, σo/Mr
SLAB RADIUS – a, in inches
0
0.1
0.2
0.3
0.4
0.5
0.6
0.7
0.8
80
100
120
140
160
180
200
220
240
T=40
T=30
T=20
h=8"
h=10"
h=14"
h=18"

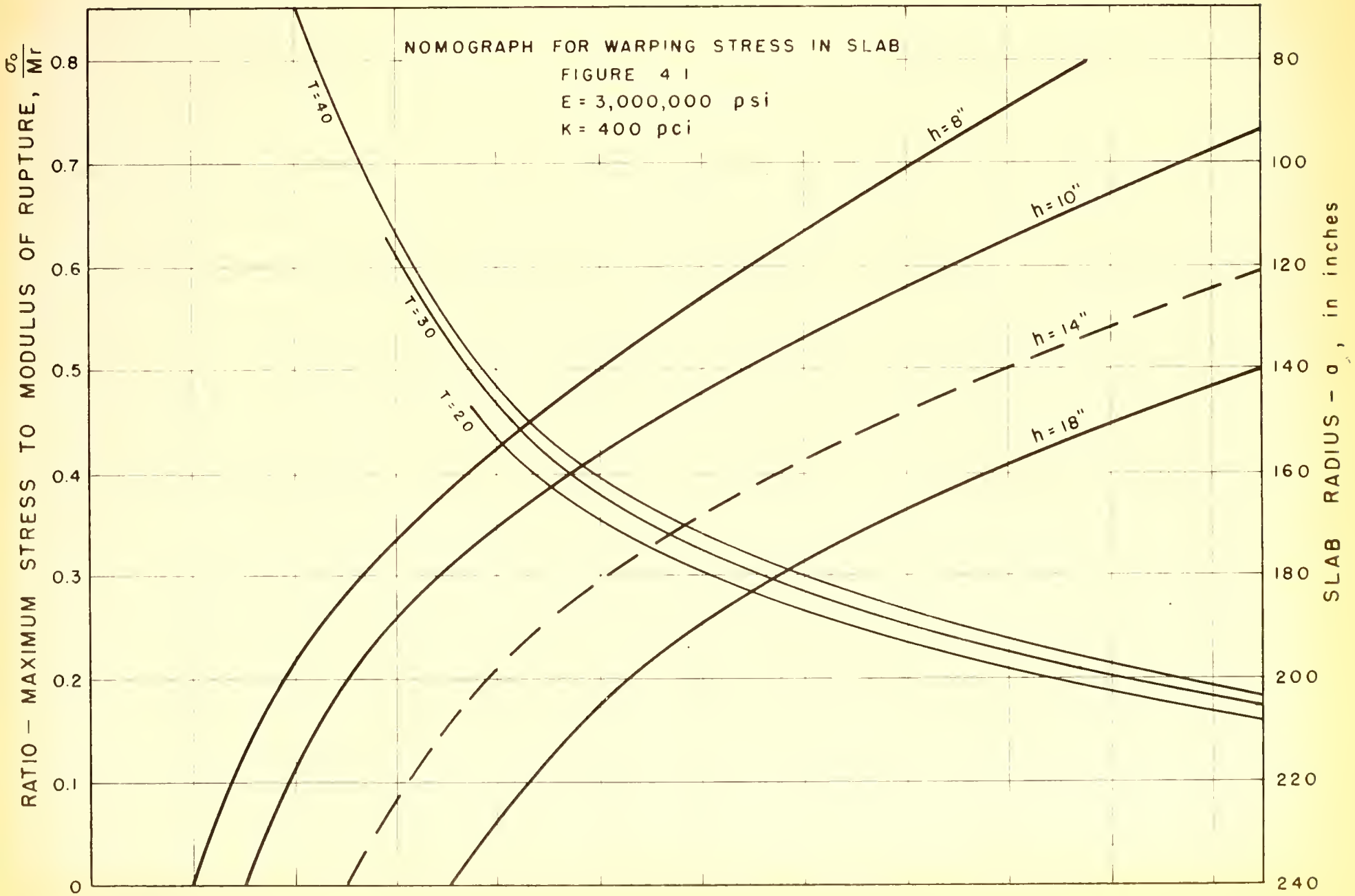
NOMOGRAPH FOR WARPING STRESS IN SLAB
FIGURE 41
E = 3,000,000 psi
K = 400 pci
RATIO – MAXIMUM STRESS TO MODULUS OF RUPTURE, $\frac{\sigma_o}{M_r}$
SLAB RADIUS – a, in inches
T=40
T=30
T=20
h=8"
h=10"
h=14"
h=18"
0
0.1
0.2
0.3
0.4
0.5
0.6
0.7
0.8
80
100
120
140
160
180
200
220
240

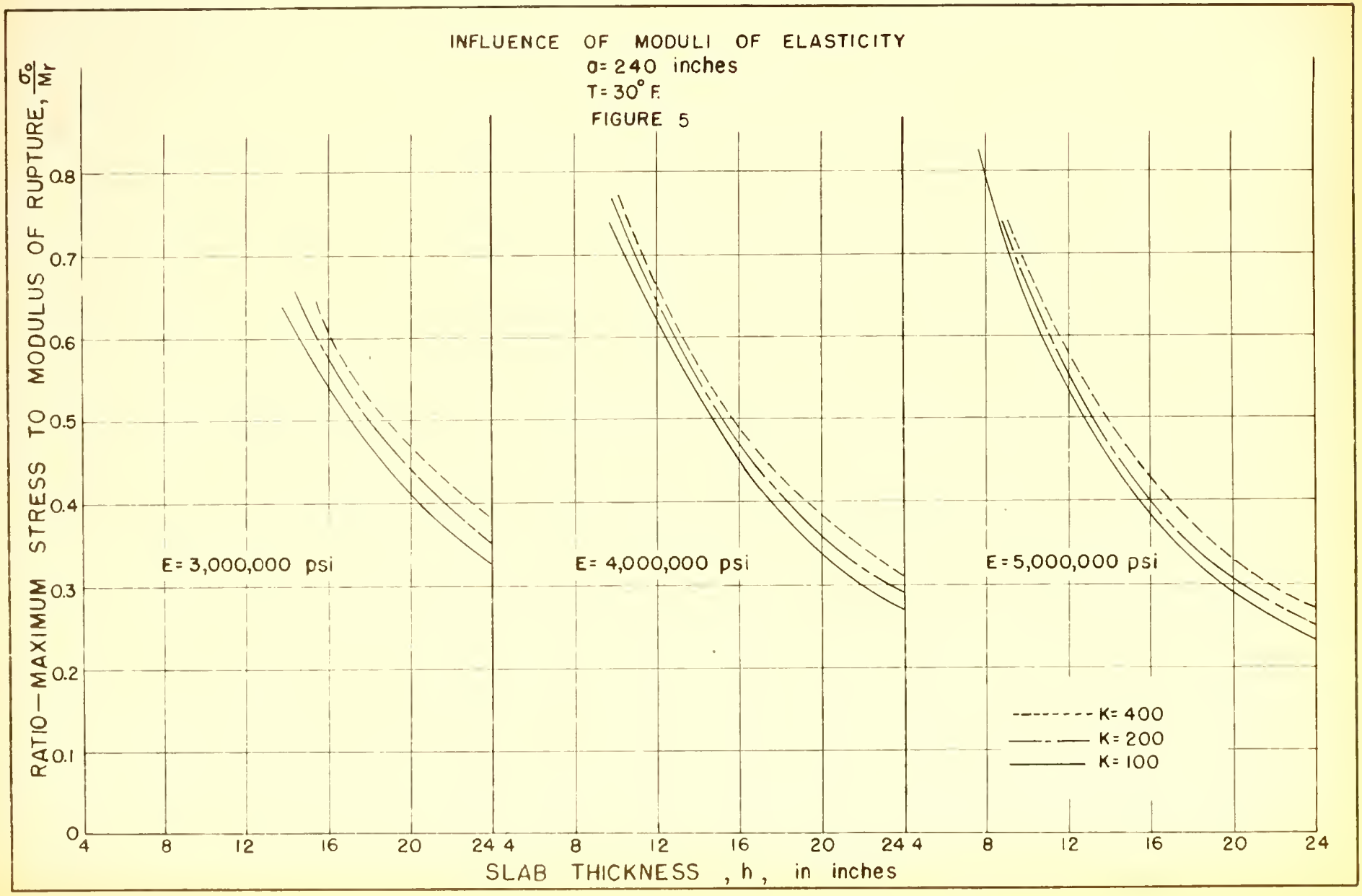
INFLUENCE OF MODULI OF ELASTICITY
a= 240 inches
T= 30° F.
FIGURE 5
RATIO—MAXIMUM STRESS TO MODULUS OF RUPTURE, $\frac{\sigma_o}{M_r}$
0
0.1
0.2
0.3
0.4
0.5
0.6
0.7
0.8
E= 3,000,000 psi
E= 4,000,000 psi
E= 5,000,000 psi
K= 400
K= 200
K= 100
4
8
12
16
20
24
SLAB THICKNESS , h , in inches

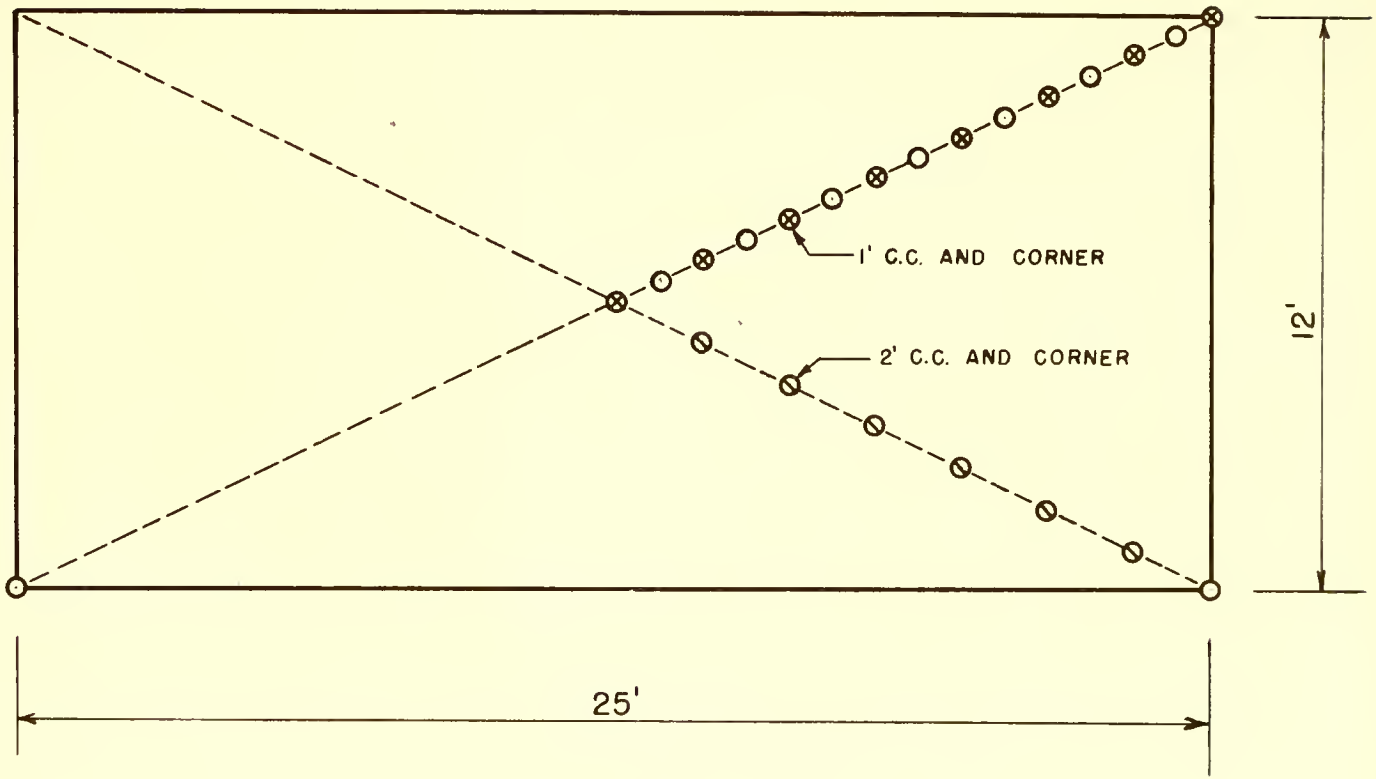

FIGURE 6

LOCATION OF DEFLECTION MEASUREMENTS

LEGEND

× = MICROMETER WITH DEEP REFERENCE RODS

\ = MICROMETER WITH SHALLOW REFERENCE RODS

O = SURFACE DIAL GAUGES

FIGURE 7

EXPERIMENTAL SLAB
PORTLAND CEMENT ASSOCIATION

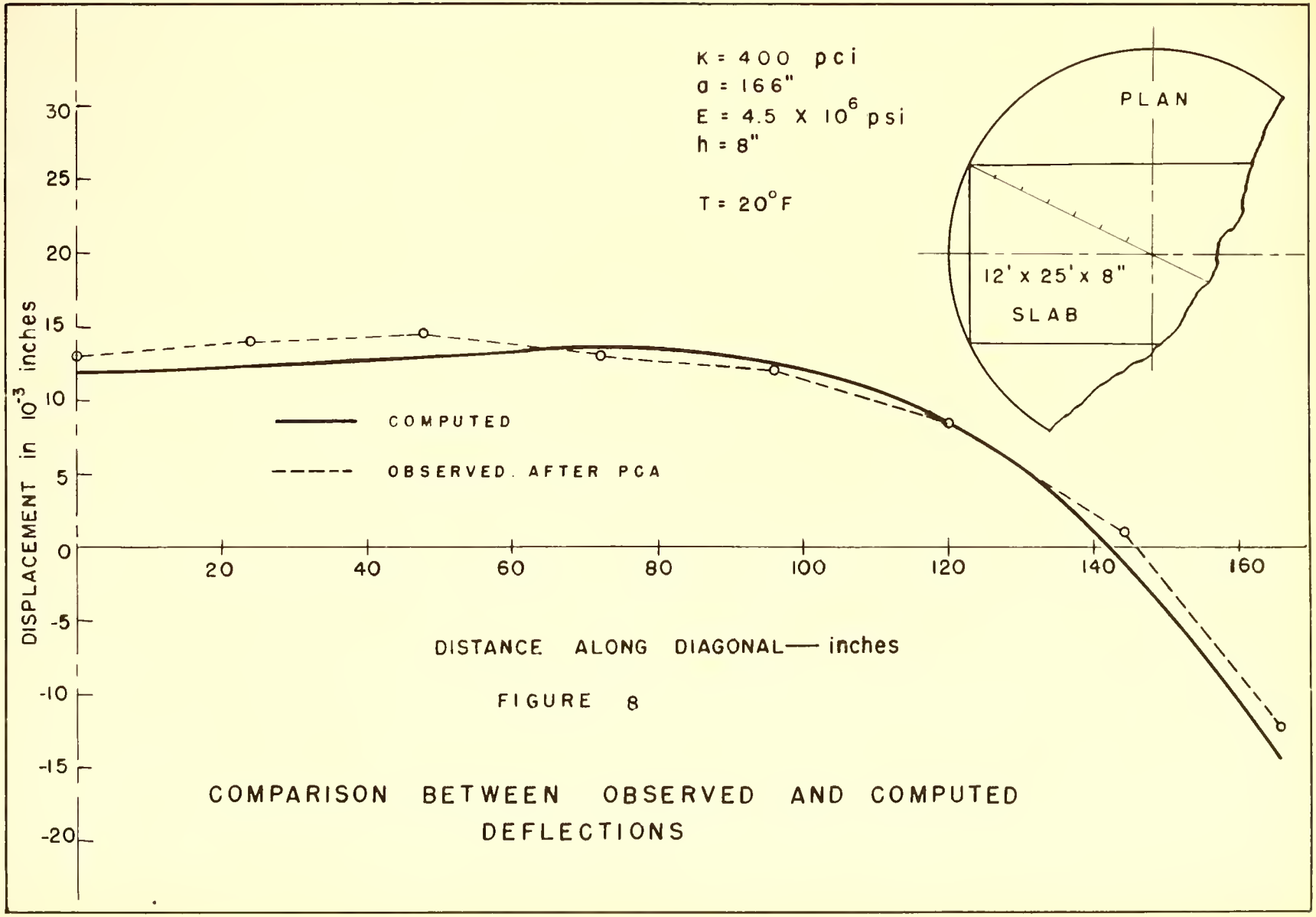

FIGURE 8

COMPARISON BETWEEN OBSERVED AND COMPUTED DEFLECTIONS

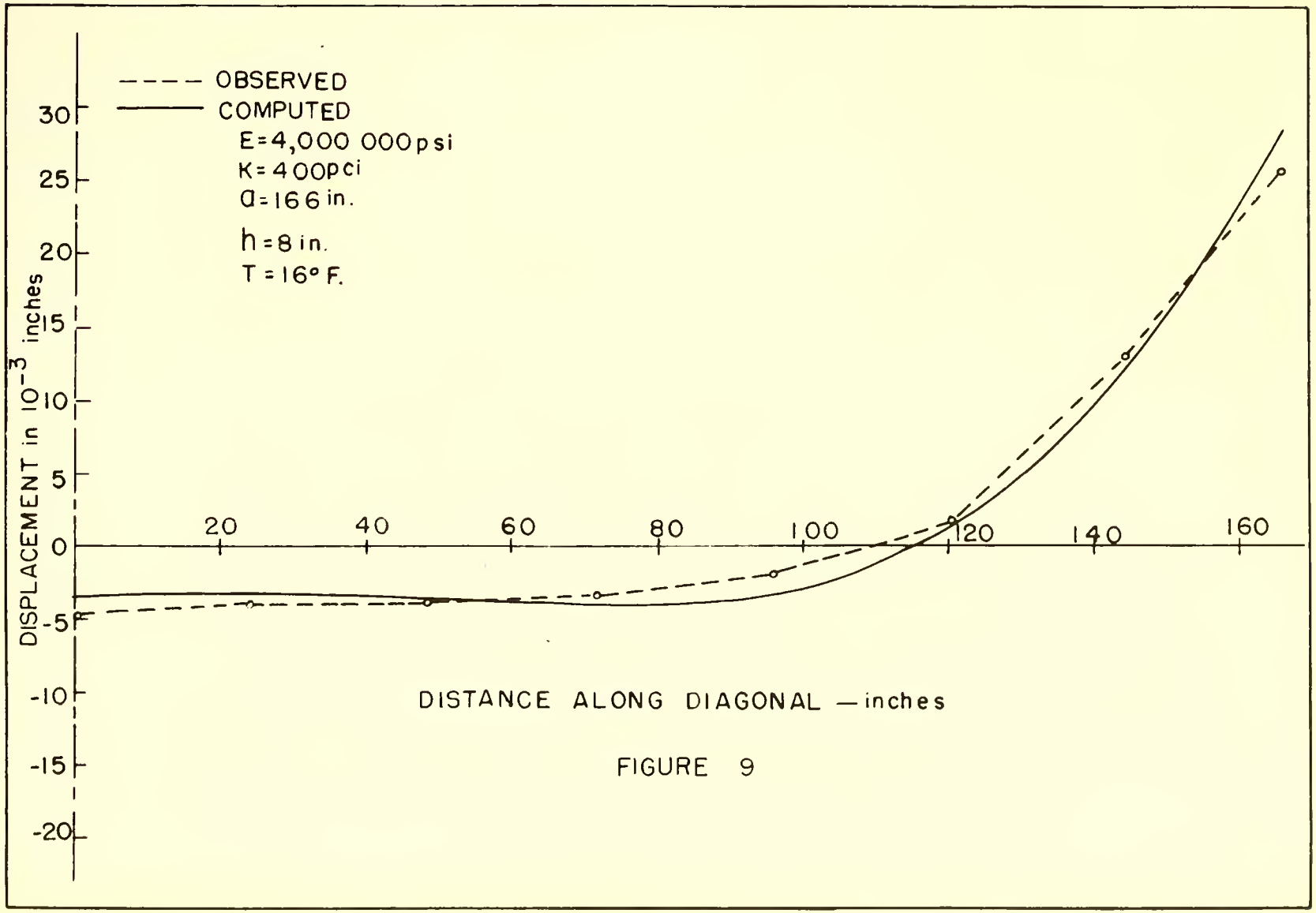
OBSERVED
COMPUTED
E=4,000 000psi
K=400pci
a=166 in.
h=8 in.
T=16° F.
DISPLACEMENT in 10^{-3} inches
30
25
20
15
10
5
0
-5
-10
-15
-20
20
40
60
80
100
120
140
160
DISTANCE ALONG DIAGONAL — inches

FIGURE 9